Ettingshausen and Nernst effects in mixed state of YBa_2Cu_30_<7-δ>(High Field Superconductors)

著者	Sasaki Takako, Watanabe Kazuo, Kobayashi Norio
journal or publication title	Science reports of the Research Institutes, Tohoku University. Ser. A, Physics, chemistry and metallurgy
volume	42
number	2
page range	351-358
year	1996-07-15
URL	http://hdl.handle.net/10097/28629

Sci. Rep. RITU A42 (1996) pp. 351-358
No. 2, May 1996

Ettingshausen and Nernst effects in mixed state of $YBa_2Cu_3O_{7-\delta}$*

Takako Sasaki, Kazuo Watanabe and Norio Kobayashi

Institute for Materials Research, Tohoku University, Sendai 980-77, Japan

(Received February 19, 1996)

The dissipative behaviors under the Lorentz force and the thermal force are investigated for the same sample of QMG-$YBa_2Cu_3O_{7-\delta}$ by measuring the Ettingshausen and the Nernst effects, respectively, and compared with each other. The value of $S_\phi(T)$ obtained from the Nernst effect is found to be smaller than that obtained from the Ettingshausen effect, which suggests that the viscosity is not the same for the vortex motions under the Lorentz force and the thermal force. The QMG-$YBa_2Cu_3O_{7-\delta}$ always includes precipitates of Y_2BaCuO_5 phase which are finely dispersed by an addition of Pt. In order to investigate the effect of Y_2BaCuO_5 phase on the vortex motion, the Ettingshausen effect is also measured for the sample with 0.5 mass% Pt addition. The anisotropy of the dissipation under the thermal force is investigated by measuring the Nernst effect for the configurations; (1) $H//c$, $(dT/dx)//ab$, (2) $H//ab$, $(dT/dx)//ab$ and (3) $H//ab$, $(dT/dx)//c$. For these vortex motions, viscosities are found to be in the ratio 30:1:100. The velocity of vortices is estimated from the Nernst field. Furthermore, using $S_\phi(T)$ the magnitude of viscosity is estimated to be $0.5\text{-}3\times10^{-7}$ N s/m^2 in the temperature range from 90 to 75 K and the magnetic field of 13 T parallel to the c-axis.

KEYWORDS: $YBa_2Cu_3O_{7-\delta}$, Ettingshausen effect, Nernst effect, vortex motion, transport entropy of a vortex

1. Introduction

Most of the studies on the dissipation in the mixed state of high T_c superconductors (HTSC) have been performed by the electrical resistivity measurement where the Lorentz force acts on a vortex as a driving force. The dissipation caused by the Lorentz force usually depends on the relative orientation of the applied magnetic field with respect to the transport current. However, in strongly anisotropic superconductors ($\gamma=\xi_{ab}/\xi_c \gg 1$, where ξ_{ab} and ξ_c are the coherence lengths parallel to the *ab*-plane and the *c*-axis), the dissipation is dominated by the direction of the magnetic field to the CuO_2 layers (not to the transport current), that is, it is independent of the Lorentz force[1-4]. Because of the large anisotropy and the small coherence length, the superconducting fluctuation becomes pronounced in HTSCs and the fluctuation effect plays an important role on the dissipation around T_c. Under the magnetic field this effect becomes more pronounced and then becomes important in a wider temperature range around $T_{c2}(H)$. The Lorentz force independent dissipation is also considered to be related with the superconducting fluctuation[5]. Moreover, relating to the anisotropy and the small coherence length, many intaresting phenomena on the vortex state or dynamics, that is, the vortex glass, vortex lattice melting, thermal depinning and so on, are revealed in HTSCs. In usual, the electrical resistivity, thermopower or Hall effect are measured in order to investigate the transport properties in the mixed state of HTSCs. However, these physical quantities always include the normal state contributions around T_c. Therefore, these measurements are not always fit for the study of the vortex motion. There is a further class of experiments where the thermal diffusion of a vortex is caused by the temperature gradient. The vortex motion under the thermal force results in the Nernst effect. Furthermore, the Ettingshausen effect, which is a reciprocal phenomenon of the Nernst effect, is caused by the vortices driven by the Lorentz force, where vortices transport the entropy and yield a transverse temperature gradient across the sample. Since the thermomagnetic effects are conspicuous only in the superconducting transition region, these effects make possible to study the dissipation phenomena by the vortex motion with great accuracy even at the temperatures around T_c, and lead to the determination of important parameters such as the transport entropy of a vortex.

In this paper, the vortex motion is investigated for $YBa_2Cu_3O_{7-\delta}$ samples (#A, #B and #C) prepared by the quench and melt growth (QMG) method[6]. In order to compare the dissipations caused by the thermal force with that caused by the Lorentz force, the Ettingshausen and Nernst effects are measured for sample #A at magnetic fields parallel to the *c*-axis. From both effects the transport entropies are estimated respectively. The QMG-$YBa_2Cu_3O_{7-\delta}$ which always includes precipitates of Y_2BaCuO_5 phase is the most promising for technical applications. The Y_2BaCuO_5 phase is finely dispersed by an addition of Pt. Those precipitates are expected to be effective pinning center.s. In order to investigate the effect of Y_2BaCuO_5 phase on the vortex motion, the Ettingshausen effect is also measured for sample #B with 0.5mass % Pt addition. The anisotropy of the vortex motion caused by the thermal force is investigated for sample #C by measuring the Nernst effect. Furthermore, the velocity of the vortex motion is estimated from the Nernst field.

*IMR, Report No. 2045

2. Experimental

2-1. Theoretical Background

The Ettingshausen effect is caused by the vortices driven by the Lorentz force. Under a magnetic field oriented in the z-direction, the transport current, J_x, passing through the superconductor in the mixed state exerts the Lorentz force, $F^L=J_x\times\Phi_0$, on a vortex. The moving vortices carry the entropy per unit length of a vortex line, S_ϕ, and result in a heat flow, $U_\kappa=n\,T\,S_\phi\,v_\phi$, in the y-direction, where $n=B_z/\Phi_0$ is the density of vortex and v_ϕ the vortex velocity. This heat flow is compensated by the heat conduction $U_\kappa=\kappa(dT/dy)$ with the thermal conductivity κ, resulting a temperature gradient dT/dy across the sample. The vortex motion with the velocity v_ϕ induces the longitudinal electric field $E_\phi=B_z\times v_\phi$. The electrical resistivity ρ_ϕ is then expressed by $\rho_\phi=E_\phi/J_x$. Combining this with the equation of the heat flow, the transport energy of a vortex line is written as

$$U_\phi=\mathrm{T}\,S_\phi=\Phi_0\,\kappa(dT/dy)/(\rho_\phi\,J_x). \quad (1)$$

The vortex motion by the thermal force leads to the Nernst effect. Since a vortex has a large entropy compared to the superconducting surrounding, the temperature gradient dT/dx applied in the x-direction yields a thermal force, $F^{TH}=-S_\phi(dT/dx)$, acting on a vortex. Vortices experiencing the thermal force move from the hot to the cold end of the sample with a velocity v_ϕ and the vortex motion results in the transverse electric field $E_y=-v_\phi B_z$, namely the Nernst field. The thermal force is balanced with the viscous drag force $F^\eta=\eta\,v_\phi$. Then we get

$$-S_\phi(dT/dx)-\eta\,v_\phi=0, \quad (2)$$

where η is a coefficient of viscosity. Inserting $-v_\phi=E_y/B_z$ into eq. (2), the normalized Nernst field is obtained to

$$E_y/(dT/dx)=S_\phi\,B_z/\eta. \quad (3)$$

The value of η can be obtained from the flow resistivity. Inserting $v_\phi=J_y\,\rho_\phi/B_z$ into the balance equation between the Lorentz force and the viscous drag force, $J_y\times\Phi_0=\eta\,v_\phi$, we get

$$\eta=\Phi_0\,B_z/\rho_\phi, \quad (4)$$

where the vortices move toward the x-direction. Combining eqs. (3) and (4), S_ϕ is given by

$$S_\phi=(\Phi_0/\rho_\phi)[E_y/(dT/dx)]. \quad (5)$$

Since the Ettingshausen and the Nernst effects are reciprocal phenomena each other, these effects are expected to give the same value of S_ϕ.

2-2. Samples

Three kinds of samples of $YBa_2Cu_3O_{7-\delta}$ were prepared by the quench and melt growth (QMG) method. In the QMG method a small amount of Pt is usually added in order to disperse the Y_2BaCuO_5 (211) phase finely and to introduce the effective pinning center. Sample #A was grown without Pt addition to avoid introducing further extrinsic pinning center as possible. This sample was used for the measurement of the Ettingshausen and the Nernst effects at the magnetic field parallel to the c-axis ($H//c$). Other two samples (sample #B and #C) were made by the usual QMG method with 0.5 mass% Pt. addition The Ettingshausen effect was also measured for the sample #B. The sample #C was used to investigate the anisotropy of the Nernst effect.

The electrical resistivities of samples #A and #B exceed 500 μΩcm at 110 K. Whereas, sample #C exhibits lower resistivity of about 83 μΩcm at 110 K, which means that this sample includes less structural defects such as a macro- and micro- cracks. Therefore, sample #C is the most suitable for measurement of the anisotropy among these three samples.

2-3. Experimental Procedure

The Ettingshausen effect was measured by a quasi-steady state technique in the configuration of $H//c$-axis (z-direction) and $J//ab$-plane (x-direction). The temperature of the heat bath was increased continuously at a slow rate of 30-80 mK/min using a capacitance temperature controller. The transverse temperature gradient dT/dy was measured by a differential chromel-constantan (CRC) thermocouple for electrical currents alternately changed with a time interval of 3 minutes, and was determined from the antisymmetric part of measured signal as $dT/dy=[dT/dy(+J)-dT/dy(-J)]/2$. The electrical resistivity was measured by a conventional four-prove method and determined as $\rho=[E_x(+J)-E_x(-J)]/2J$. The CRC thermocouple was confirmed not to be influenced by magnetic fields up to 14 T between 30 and 110 K within an experimental accuracy of ±3 %.

The Nernst effect and thermal conductivity were measured by a steady-state technique. The temperature gradient dT/dx was also detected by a CRC differential thermocouple. The Nernst voltage was measured for two opposite directions of a magnetic field to eliminate any other contributions such as a thermoelectric voltage in the leads and so on. The normalized Nernst field was determined as $E_y/(dT/dx)=[E_y(+H)-E_y(-H)]/2(dT/dx)$. The experimental technique was reported in detail elsewhere.[7]

3. Result and Discussion

3-1. Ettingshausen Effect

3-1-a. Ettingshausen effect for $H//c$-axis[7]

The vortex motion caused by the Lorentz force has been investigated by measuring the Ettingshausen effect for sample #A at the magnetic field $H//c$-axis and the transport current $J//ab$-plane. In the flux flow state, dT/dy caused by the Ettingshausen effect is expected to be proportional to the applied current. The linear response of dT/dy to currents of 25-100 mA was experimentally confirmed. In the following experiments, the transport current of 100 mA (J=5.68 A/cm^2) is used to ensure sufficient accuracy of dT/dy. If the current is increased more than 100 mA, the Joule heating at electrodes becomes too large to be ignored. Figure 1 (a) shows dT/dy as a function of temperature for different magnetic fields. The corresponding electrical resistivity is shown in Fig. 1(b). As expected, a finite value of dT/dy is observed in the superconducting transition region. The value of dT/dy takes a maximum around a midpoint of the resistive transition, which can be explained by the competition between the increase in v_ϕ and the decrease in S_ϕ with increasing temperature. The magnetic field dependence of dT/dy is shown in Fig. 2. As shown in this figure, dT/dy also has a maximum as a function of magnetic field, which is caused by the competition between the increase in the density of

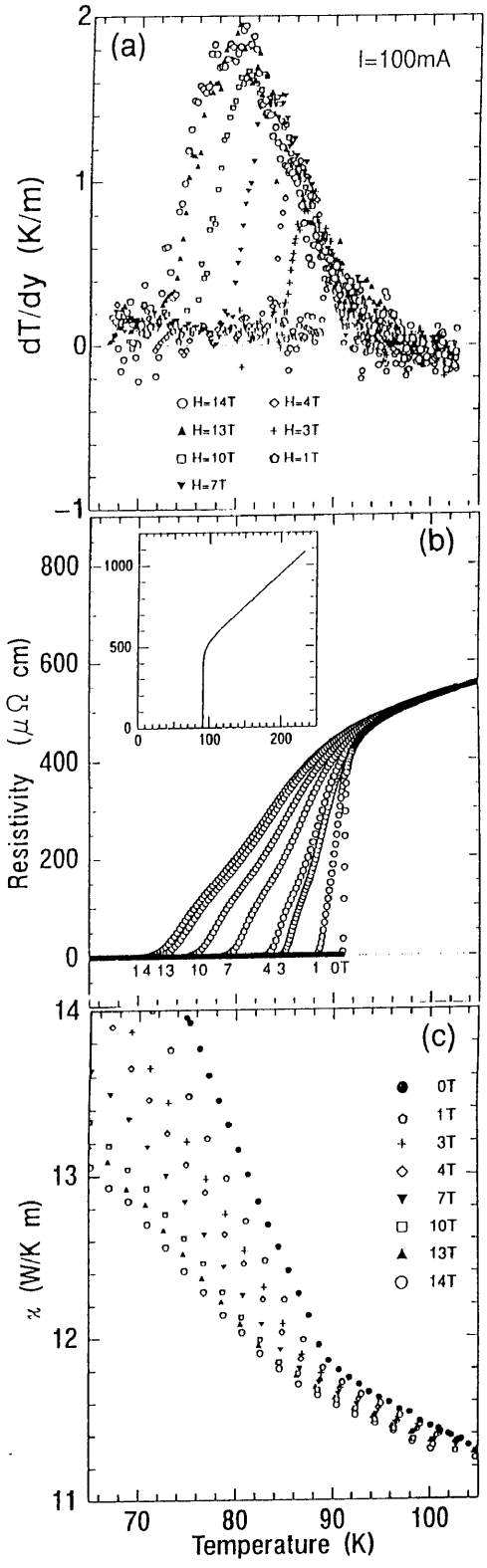

Figure. 1. Temperature dependence of (a) transverse temperature gradient dT/dy, (b) longitudinal electrical resistivity ρ, and (c) thermal conductivity κ for sample #A.

vortex $n=B_z/\Phi_0$ and the decrease in S_ϕ with increasing magnetic field.

3-1-b. Transport energy[7]

According to eq. (1), the transport energy $U_\phi=TS_\phi$ is calculated using dT/dy, ρ_ϕ and κ. The temperature dependence

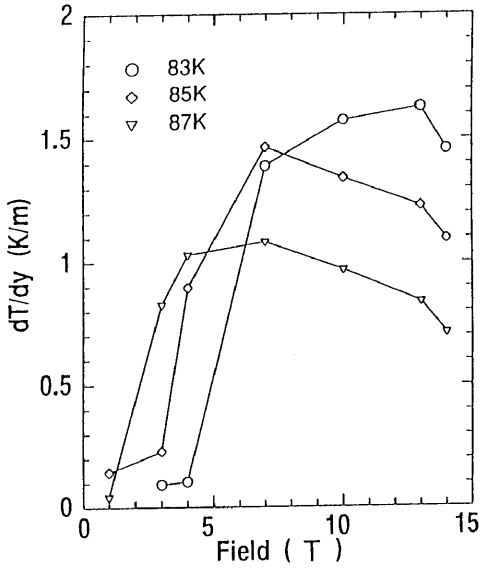

Figure. 2. Magnetic field dependence of dT/dy for sample #A at fixed temperatures of T=83. 85 and 87 K.

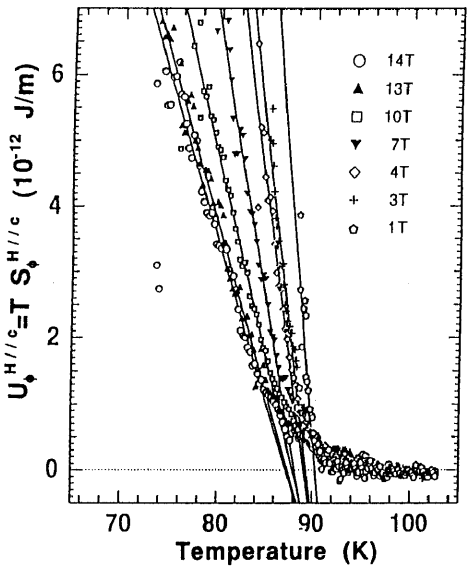

Figure. 3. Temperature dependence of transport energy $U_\phi^{H//c}$ estimated from Ettingshausen effect for sample #A.

of κ is shown in Fig.1 (c). As shown in Fig. 1 (a), the normal state resistivity just above T_c is about 500 μΩcm. Samples made by the QMG method usually include macro- and micro cracks and 211-phase precipitates. These structural defects contribute to the electron scattering and lead to an increase of the resistivity. Therefore, the resistivity measured in a magnetic field can not be regarded as only due to the flux flow. In this paper, for convenience, we assume that the flow resistivity generated in the QMG sample is of the same order as the resistivity measured in a single crystal in which the extrinsic contribution to the resistivity might be very small. The flow resistivity in sample #A (and also in #B) is estimated as

$\rho_\phi(T, H)=\rho(T, H)/[\rho(100\ K)/\rho_s(110\ K)]$, where $\rho_s(110\ K)$=55 μΩcm is the resistivity of the single crystal at 100 K and 0T reported by Palstra et al[8].

The temperature dependence of U_ϕ is shown in Fig. 3.

On the basis of the time dependent Ginzburg-Landau (GL) theory, Maki obtained the theoretical expression for U_ϕ [9,10] as follows:

$U_\phi(T)=(\Phi_0/4\pi)\{(H_{c2}(T)-H)/[1.1682(\kappa_{GL}^2-1)+1]\}L_D(T)$, (6)

where $L_D(T)$ is a numerical function increasing monotonically from 0 to 1 with increasing temperature, which is about 1 for close to T_c, and κ_{GL} is the Ginzburg-Landau parameter. Equation (6) predicts that for a constant applied magnetic field, dU_ϕ/dT is constant in the temperature range close to T_c, since according to the GL theory, dH_{c2}/dT=constant and the temperature dependence of L_D is negligible near T_c. Furthermore, dU_ϕ/dT dose not depend on the applied magnetic field. As shown in Fig. 3, the former property is clearly observed. However, the latter cannot be recognized experimentally. The experimental result shows a decrease of $-dU_\phi/dT$ with increasing magnetic field. The disagreement between the experimental result and theoretical prediction may arise from the superconducting fluctuation effect[11,12] which increases with increasing magnetic field and/or increasing temperature. This fluctuating effect enhances U_ϕ more remarkably at higher magnetic fields and/or higher temperatures and would be expected to result in a decrease of the slope of $U_\phi(T)$ with increasing magnetic field. In the system where the fluctuation is stronger, namely in two dimensional system, even the linearity of $U_\phi(T)$ would not be held in wider temperature range

According to eq. (6), $T_{c2}(H)$ and hence $H_{c2}(T)$ can be derived by the extrapolation of the linear part of $U_\phi(T)$ to zero. The temperature dependence of H_{c2} obtained from Fig. 3 is almost linear with $dH_{c2}/dT\approx$-5 T/K which results in a coherence length of $\xi(0)\approx$11 Å at T=0 K. Equation (6) yields $\kappa_{GL}=\sqrt{(\Phi_0/9.28\pi)[(dH_{c2}/dT)/(dU_\phi/dT)]}$. This equation gives $\kappa_{GL}\approx$80, using the values of $-dU_\phi/dT=5\times10^{-13}$ J/K at 13 T and $dH_{c2}/dT\approx$5 T/K.

3-1-c. Effect of Y_2BaCuO_5 phase on vortex motion[7]

Bulk samples prepared by the QMG method always contain a considerable amount of Y_2BaCuO_5 (211) phase. The addition of Pt serves to disperse the 211-phase finely. The fine precipitates are expected to be effective on the vortex pinning. In order to investigate the effect of the size of 211-phase precipitates on the vortex motion, the Ettingshausen effect was also measured for sample #B with Pt addition. The temperature dependence of dT/dy is shown in Fig. 4 (a). The values normalized by the current density J=6.94 A/cm^2 are smaller than that obtained for sample #A. For example, the maximum value of $(dT/dy)/J$ at 14 T is about 30 % smaller . According to eq. (1), $(dT/dy)/J$ is proportional to U_ϕ, $1/\kappa$ and ρ_ϕ. As one can see by comparing Fig. 1 (c) with Fig. 4 (c), κ for sample #B is about 37 % smaller than that for sample #A, which leads to rather a larger value of $(dT/dy)/J$ in sample #B in contradiction to the experimental result. Therefore, the decrease of $(dT/dy)/J$ with addition of Pt is considered to arise from decrease of ρ_ϕ, i.e. lowering of the vortex velocity, and/or suppression of U_ϕ. The measured value of ρ for sample #B is larger than that for sample #A. However, as mentioned before, ρ can not be regarded as ρ_ϕ because of a excessive component caused by other resistive mechanisms. In the QMG-

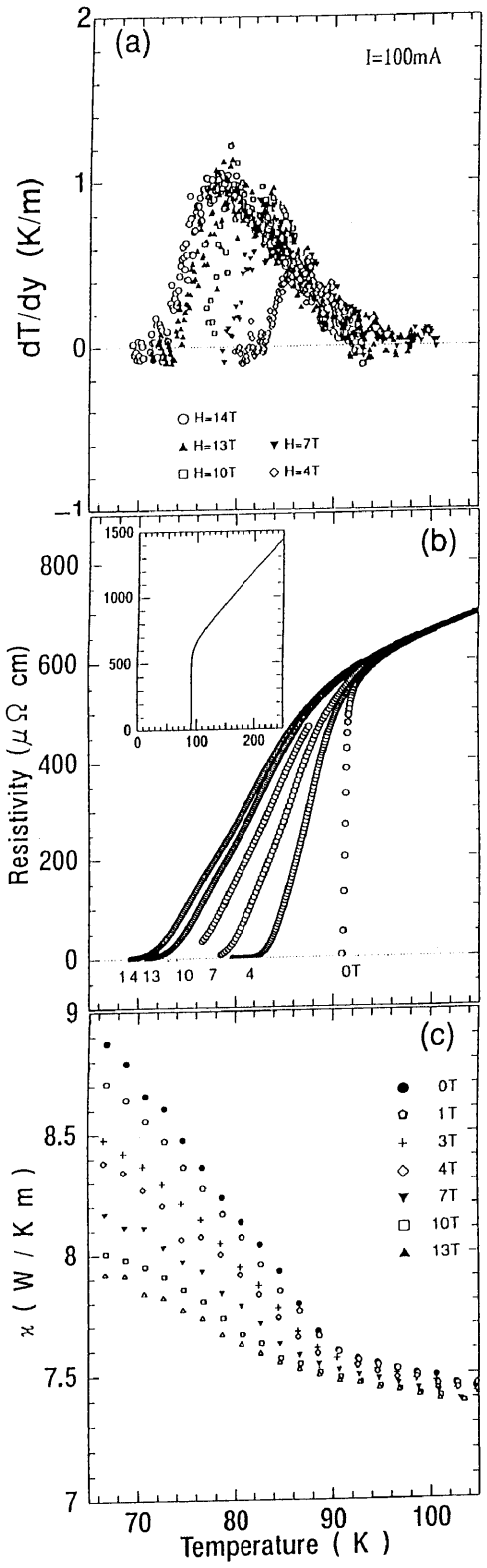

Figure. 4. Temperature dependence of (a) transverse temperature gradient dT/dy , (b) longitudinal electrical resistivity ρ, and (c) thermal conductivity κ for sample #B.

$YBa_2Cu_3O_{7-\delta}$ samples, the effective pinning sites are the precipitates of the 211-phase as well as defects, oxygen deficiency, twin boundary and dislocation. The dc magnetization measurement indicates that the critical current density increases with decreasing particle size of 211-phase.[13] Therefore it is likely that the finely dispersed 211-phase results in the reduction of the vortex velocity and hence of

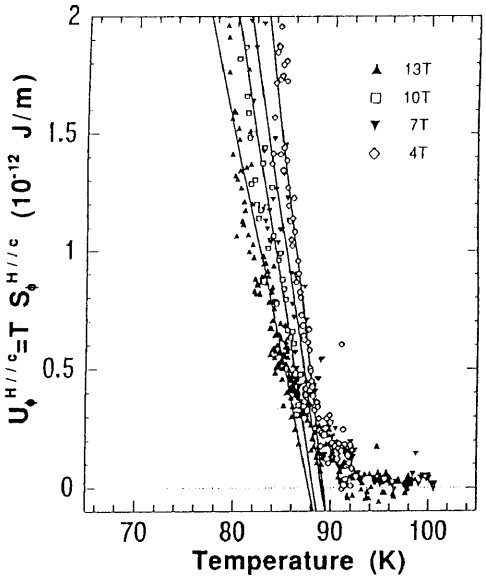

Figure. 5. Temperature dependence of transport energy $U_\phi^{H/c}$ estimated from Ettingshausen effect for sample #B.

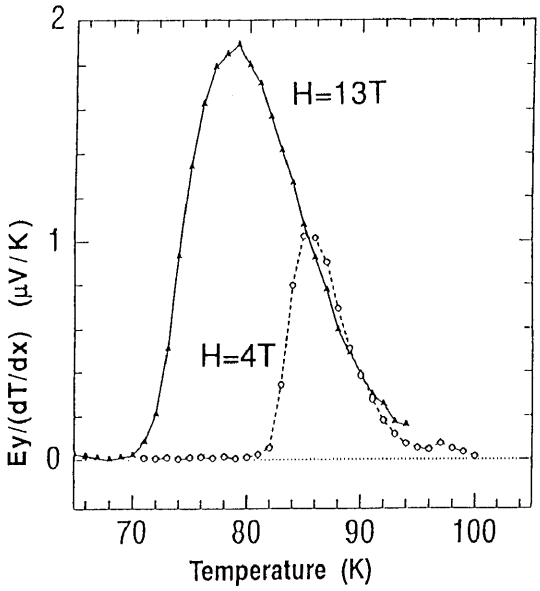

Figure. 6. Temperature dependence of normalized Nernst field $E_y/(dT/dx)$ in the configuration of $H//c$ and $dT/dx//ab$ for sample #A.

density increases with decreasing particle size of 211-phase.[13] Therefore it is likely that the finely dispersed 211-phase results in the reduction of the vortex velocity and hence of $(dT/dy)/J$. Assuming $\rho_\phi(T, H)=\rho(T, H)/[\rho(100\ K)/\rho_s(110\ K)]$ with $\rho_s(110\ K)=55\ \mu\Omega cm$, U_ϕ is estimated as a function of temperature, which is shown in Fig. 5. The value of U_ϕ is about 45 % smaller than that for sample #A. This small value may also lead to the suppression of $(dT/dy)/J$, although the U_ϕ value includes large ambiguity because of the uncertainty of ρ_ϕ.

3-2. Nernst Effect

3-2-a. Nernst effect at $H//c$-axis[7]

In order to investigate the dissipation caused by the thermal force in comparison with that caused by the Lorentz force, the Nernst effect has been measured for sample #A at magnetic fields of 4 and 13 T parallel to the c-axis. The temperature gradient $dT/dx\approx1.2$ K/cm was applied parallel to the ab-plne. The normalized Nernst field $E_y/(dT/dx)$ is shown in Fig. 6. The temperature dependence of $E_y/(dT/dx)$ is similar to that of dT/dy caused by the Ettingshausen effect, i.e. the finite Nernst field is observed in the resistive transition temperature region and takes a maximum around 80 and 86 K at 4 and 13 T, respectively. According to eq. (5), the transport energy U_ϕ is obtained from $E_y/(dT/dx)$ and ρ_ϕ. The temperature dependence of U_ϕ is shown in Fig. 7. The magnitude of U_ϕ is about 3×10^{-12} J/m at 13 T and 76 K, which is about a half of U_ϕ estimated from the Ettingshausen effect (see curves A and A' in Fig. 11). According to the Bridgman relation, however, U_ϕ obtained from the Nernst effect should be the same as that obtained from the Ettingshausen effect. We here consider the origin of the discrepancy. When we estimated U_ϕ from the Nernst effect according to eq. (4), the value of η obtained from ρ_ϕ was used. However, this may not be correct if the viscosity of the vortex motion caused by the thermal force is not the

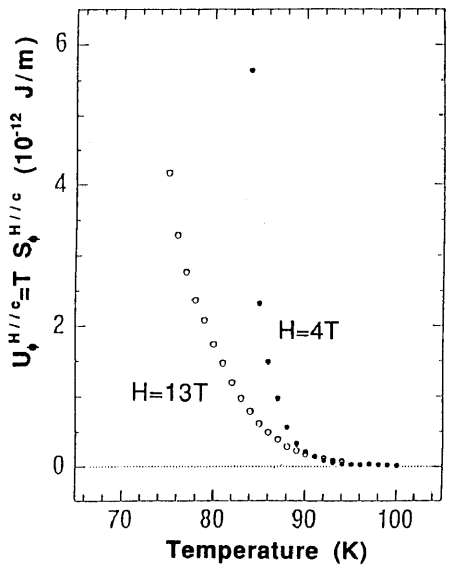

Figure. 7. Temperature dependence of transport energy $U_\phi^{H/c}$ estimated from the Nernst effect for sample #A.

same as that under the Lorentz force. Because of two-dimensionality of the material, there is a finite probability of the thermal creation of vortex-antivortex (V-AV) pairs.[14-16] It should be noted that vortex and antivortex driven by the Lorentz force move in the opposite directions each other and generate a finite longitudinal resistivity, whereas the thermal force acts in the same direction for both vortex and antivortex. Therefore, V-AV pairs cannot contribute to the time averaged Nernst voltage. In such a situation, it is doubtful whether the value of η calculated in eq. (4) is also applicable to the vortex motion under the thermal force. In order to clarify the origin of the discrepancy, further study is needed, for example, measurements of both effects for a single crystal without other components in ρ.

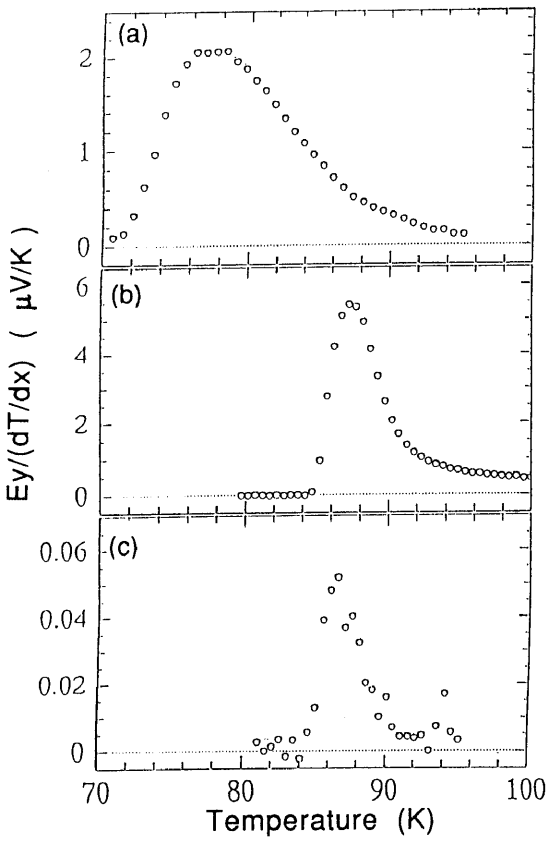

Fig.ure 8. Temperature dependence of Nernst field for configurations (a) *H//c*, (d*T*/d*x*)//*ab*, (b) *H//ab*, (d*T*/d*x*)//*ab* and (c) *H//ab*, (d*T*/d*x*)//*c* for sample #C.

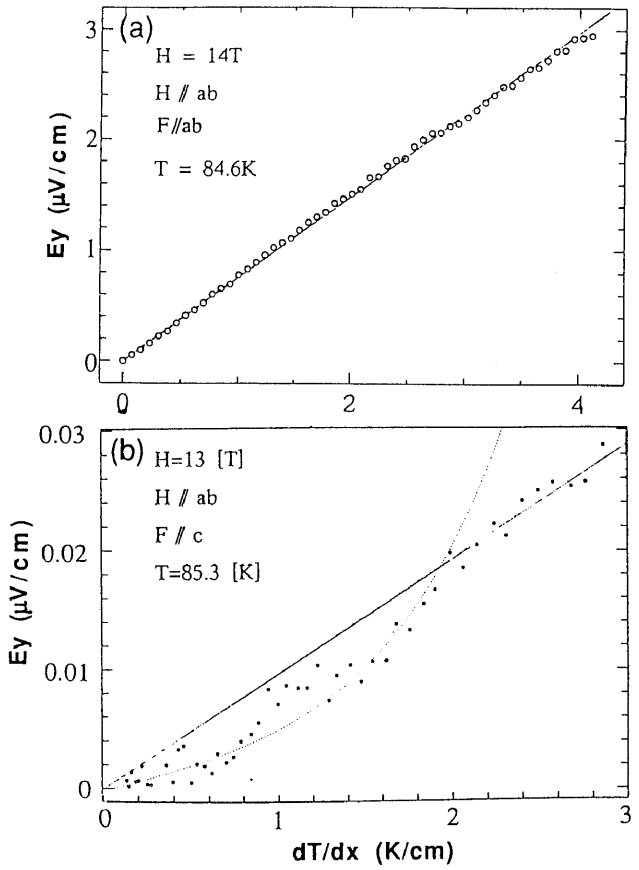

Figure. 9. E_y-dT/dx characteristics for sample #C at a magnetic field parallel to the ab-plane. Lateral motion at H=14 T (a) and longitudinal motion at H=13T(b).

3-2-b. Anisotropy of Nernst effect[17)]

In order to investigate the anisotropy of the vortex motion, the Nernst effect has been measured for sample #C at magnetic field of 13 T for three configurations (1) *H//c*, (d*T*/d*x*)//*ab*, (2) *H//ab*, (d*T*/d*x*)//*ab* and (3) *H//ab*, (d*T*/d*x*)//*c*. The dimensions of the sample are 7.5×1.6(*a*×*b*)×10(*c*) mm^3 for the configurations (2) and (3), although a part of this sample with dimensions of 7.5×1.6(*a*×*b*)×1.0(*c*) mm^3 was used for the measurement in the configuration (1).

The temperature dependence of E_y/(dT/dx) for configurations (1) and (2) were measured applying $dT/dx \approx 1.2$ K/cm, which are shown in Figs. 8 (a) and (b). Values of E_y/(dT/dx) for the configuration (3) were measured applying a larger temperature gradient about 3 K/cm to ensure the linear response of the Nernst voltage to dT/dx. The result is shown in Fig. 8 (c). For *H//c*, the maximum value of E_y/(dT/dx) is about 2 μV/K. For *H//ab*, the magnitude of E_y/(dT/dx) is depends on the direction of the thermal force. As shown in Fig. 8 (c), vortices driven toward the *c*-axis yields only 0.06 μV/K even at the maximum, which is about 100 times smaller than that induced by the lateral motion. We estimate the anisotropy of the vortex motion using the ratio in the viscosity η. According to eq. (3), η is proportional to $S_\phi/[E_y/(dT/dx)]$. Therefore, only the ratio in $S_\phi/[E_y/(dT/dx)]$ is discussed. As for the configuration (2) and (3), the magnitude of S_ϕ is expected to be the same, since the magnetic field is parallel to the ab-plane for both configurations. Therefore, the ratio in $1/[E_y/(dT/dx)]$ directly indicates the anisotropy in η. From Figs. 8 (b) and (c), it is obtained that $\eta_c^{H//ab}/\eta_{ab}^{H//ab} \approx 100$. Here $\eta_c^{H//ab}$ and $\eta_{ab}^{H//ab}$ are viscosities in the configurations (2) and (3), respectively. When we estimate the ratio of $\eta_{ab}^{H//c}$ at the magnetic field parallel to the *c*-axis to $\eta_{ab}^{H//ab}$, it is assumed that the ratio in S_ϕ, namely $S_\phi^{H//c}/S_\phi^{H//ab}$, is given by the ratio in the magnetic penetration depth, λ_c/λ_{ab}, since the free energy of a vortex per unit length is approximately proportional to $1/\lambda^2$ when $\lambda \gg \xi$.[18)] The value of λ_c/λ_{ab} has been obtained experimentally to be about 5.[19)] From Figs. 8 (a) and (b) using $S_\phi^{H//c}/S_\phi^{H//ab} \approx \lambda_c/\lambda_{ab} \approx 5$, the ratio $\eta_{ab}^{H//c}/\eta_{ab}^{H//ab}$ is obtained to be about 25 (T=86 K) and about 47 (T=87 K). And then, for three directions of the vortex motion, it is concluded that

$$\eta_{ab}^{H//c}:\eta_{ab}^{H//ab}:\eta_c^{H//ab} \approx 30:1:100. \quad (7)$$

The anisotropy of the transport property in the mixed state has been investigated by measuring the angular dependence of the electrical resistivity. It was found that the magnetic field dependence of $\rho(\theta)$ induced by the current *J//ab* is explained by the effective mass model as follows: $\rho(\theta) \propto H(\cos^2\theta+\gamma^2\sin^2\theta)^{1/2}$ with a anisotropy parameter $\gamma=\sqrt{m_c/m_{ab}}$, where m_c and m_{ab} are the effective masses for the electron motion in the *c*-direction and within the *ab*-plane, and θ is the angular between H and *c*-axis. According to eq. (4), γ can be also expressed as follows: $\gamma=\rho^{H//c}/\rho^{H//ab}=\eta_c^{H//ab}/\eta_{ab}^{H//c}$. Therefore, the ratio in η obtained from the Nernst field gives $\gamma \approx 3$ which is somewhat small but the same order compared with $\gamma \approx 4$-8[20-21)] obtained from the resistivity measurement. Within an accuracy of the analysis, the anisotropy of the vortex transport is almost the same for

both driving forces, i.e. for the thermal and Lorentz forces. As mentioned above, γ was estimated by using only two values, namely one ratio $\eta_c^{H//ab}/\eta_{ab}^{H//c}$, therefore, there is some ambiguity. In order to determine the anisotropy with higher accuracy, more detail examination, for example the measurement of the angular dependence of the Nernst field, is needed.

The large ratio in η in the configurations (2) and (3) indicates that vortices penetrating parallel to the *ab*-plane are easy to move within a weak superconducting layer, whereas those which move across CuO_2 planes are exerted a strong viscous damping force which is about 100 times larger than that in the lateral motion. The large viscosity is considered to originate from the stacking structure constructed from the strong superconducting CuO_2 planes and the weakly superconducting layers. In order to investigate the relation between the layered structure and the vortex motion in detail, the E_y-dT/dx characteristics were measured for the lateral motion and the longitudinal motion. The results are shown in Fig. 9. In the lateral motion, as shown in Fig. 9 (a), E_y is proportional to dT/dx at the whole range of dT/dx we measured, that is, the in-plane vortex motion is viscous even at the smallest driving force, which indicates that the pinning is insignificantly weak. On the other hand, in the longitudinal motion, a deviation from the linear flux flow regime is observed for dT/dx<2 K/cm, which is approximately described by the flux creep model and indicates the existence of the effective vortex pinning. From these results, it can be said that the layered structure acts as a strong pinning center for the vortex moving across the CuO_2 planes and leads to the large viscosity in the flux flow state.

3-2-c. Velocity of vortex motion

The vortex velocity v_ϕ can be derived directly from the Nernst field E_y according to the relation $v_\phi=E_y/B_z$. In Figure 6 (a), the maximum value of $E_y/(dT/dx)$ is close to 2 μV/K, from which $v_\phi \approx 1.6\times10^{-5}$ m/s is derived as a velocity induced by a temperature gradient of 1 K/cm. The vortex velocity is an important quantity especially from the viewpoint of an application, then, we convert dT/dx to J according to the relation $J=S_\phi(dT/dx)/\Phi_0$, and estimate the velocity per a transport current of 1 A/cm^2 on the basis of the data shown in Fig. 8 (a). In order to perform it, the value of $S_\phi^{H//c}$ for sample #C has to be known. In Figure 10 the temperature dependence of $U_\phi^{H//c}=T\,S_\phi^{H//c}$ which is calculated by use of eq. (5) using the measured value $\rho(T)$ in Fig. 11 is plotted. The velocity at J=1 A/cm^2 and H=13T (H//c) is shown in Fig. 12 as a function of temperature. With increasing temperature, v_ϕ increses monotonously. The magnitude of v_ϕ is 1-5x10^{-4} m/s in the temperature range from 75 to 90 K. We estimate the velocity of the vortex motion yielded by the critical current J_c. The value of J_c at 77 K and high magnetic fields was calculated in the ideal creep-free case by K. Kimura et al,[13] where the magnetic field dependence of J_c is very weak near 10 T. Extrapolating the data to 13 T gives $J_c\sim1\times10^4$ A/cm^2 which leads to $v_\phi\sim1$ m/s. As presented here, the vortex velocity per the driving force can be derived directly from the Nernst effect if the value of S_ϕ is known. Using $S_\phi(T)$ we can also estimate the viscosity η from

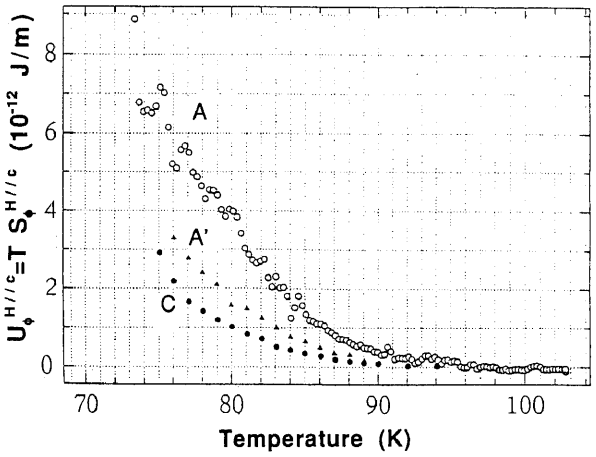

Figure. 10. Temperature dependence of transport energy $U_\phi^{H//c}$. Curves A and A' were obtained for sample #A from Ettingshausen and Nernst effects, respectively. Curve C was obtained for sample #C from Nernst effect.

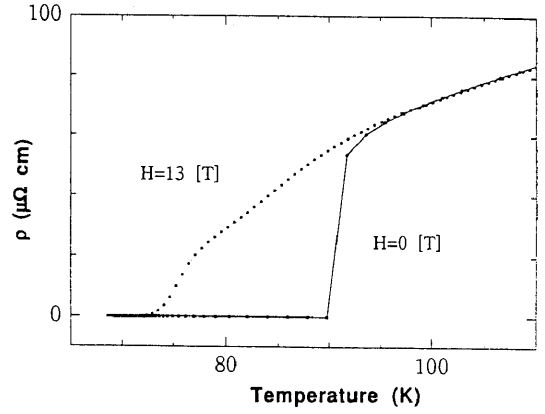

Figure. 11. Temperature dependence of longitudinal electrical resistivity ρ at H//c and J//ab for sample #C.

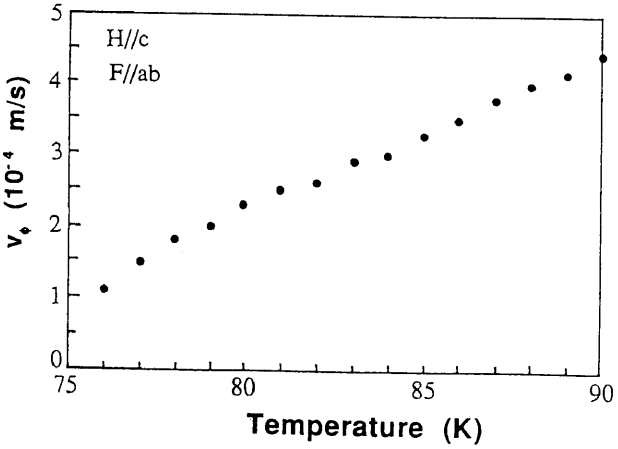

Figure. 12. Temperature dependence of vortex motion v_ϕ induced by the thermal force corresponding to the Lorentz force at H=13 T and J=1 A/cm^2.

$E_y/(dT/dx)$ according to eq. (3). With increasing temperature, as expected from $v_\phi(T)$, η decreases. The magnitude of η is estimated to be 0.5-3$\times10^{-7}$ N s/m^2 in the temperature range from 90 to 75 K.

4. Summary

The vortex motions not only under the Lorentz force but also under the thermal force have been investigated for QMG-$YBa_2Cu_3O_{7-\delta}$ by measuring thermomagnetic effects. The transport entropy is derived from both the Ettingshausen and the Nernst effects respectively. The value of $S_\phi(T)$ eatimated from the Nernst effect is somewhat smaller than that estimated from the Ettingshausen effect. This result suggests that the viscosity for the thermal force is larger than that for the Lorentz force. The magnetic field dependence of dU_ϕ/dT cannot be explained by the Maki theory. The fluctuation effect is considered to play an important role on vortex transport around T_c. In addition, important parameters, $dH_{c2}/dT \approx 5$ T/K, $\xi(0) \approx 11$ Å and $\kappa_{GL} \approx 80$, are estimated from the Ettingshauseneffect. The anisotropy of the vortex motion by the thermal force has been investigated by measuring the Nernst effect for the configurations (1) *H//c*, (d*T*/d*x*)*//ab*, (2) *H//ab*, (d*T*/d*x*)*//ab* and (3) *H//ab*, (d*T*/d*x*)*//c*. The ratio in the viscosity was obtained as follows, $\eta_{ab}^{H//c} : \eta_{ab}^{H//ab} : \eta_{c}^{H//ab} = 30:1:100$. And then, the anisotropy parameter $\gamma \approx 3$ is estimated. From the Nernst field and the transpor entropy, the viscosity at the magnetic field of 13 T parallel to the *c*-axis is estimated to be about $0.5\text{-}3\times10^{-7}$ N s/m^2 at temperatures from 90 to 75 K, which is corresponding to the vortex velocities of $1\text{-}5\times10^{-4}$ m/s at a transport current of J=1 A/cm^2.

5. Acknowledgments

This work was partialy done together with Mr. M. Sawamura and Mr. J. Ikeda of graduate student of Tohoku University. We wish to thank Dr. K. Kimura, Dr. K. Miyamoto, Dr. M. Hashimoto in Advanced Materials & Technology Research Laboratory, Nippon Steel Corporation for providing samples. We are indebted to the members of Cryogenic Center and High Field Laboratory for Superconducting Materials of Tohoku University. This work is partially supported by Grant-in Aid for Sientific Research from the Ministry of Education, Science and Culture, Japan.

1) K. Kitazawa, S. Kambe, M. Naito, I. Tanaka and H. Kojima, Jpn. J. Appl. Phys. **28**, (1989) L555.
2) Y. Iye, S. Nakamura and T. Tamegai, Physica **159**C, (1989) 433.
3) D. H. Kim, K. E. Gray, R. T. Kampwirth and D. M. Mckay, Phy. Rev. B**42**, (1990) 6249.
4) K.Kadowaki, J. N. Li and J. J. M. Franse, J. Magn. Magn. Mater. **90&91**, (1990) 678.
5) K. Kadowaki, S. L. Yuan, K. Kishio, T. Kimura and K.Kitazawa, Phy. Rev. B**50**, (1994) 7230.
6) M. Kimura, M. Tanaka, H. Horiuchi, M. Morita, M. Tanaka, M. Matsuo, M. Morikawa and K. Sawano, Physica C**175**, (1991) 262.
7) T. Sasaki, M. Sawamura, S. Awaji, K. Watanabe, N. Kobayashi, K. Kimura, K. Miyamoto and M. Hashimoto, Jpn. J. Appl. Phys. **35**, (1996) 82.
8) T. T. M. Palstra, B. Batlogg, L. F. Schneemeyer and J. V. Waszczak, Phys. Rev. Lett. **64**, (1990) 3090.
9) K. Maki, J. Low Temp. Phys. **1**, (1969) 45.
10) C.Caroli and K.Maki, Phys. Rev. **164**, (1969) 591.
11) S. Ullah and A. T. Dorsey, Phys. Rev. Lett. **65**, (1990) 2066.
12) S. Ullah and A. T. Dorsey, Phys. Rev. B**44**, (1991) 262.
13) K. Kimura, K. Miyamoto, M. Hashimoto and T. Matsushita, Trans. Inst. Electr. Eng.. Jpn **115-A No.3** (1995) 245.
14) A. M. Kadin, K. Epstein and A. M. Goldmann, Phys. Rev. B **27**, (1973) 6691.
15) J .M .Kosterlitz and D. J. Thouless, J. Phys. C **6**, (1973) 1181.
16) P. Minnhagen, Rev. Mod. Phys. **59**, (1987) 1001.
17) T. Sasaki, J. Ikeda, K. Yamada, T. Naito, K. Watanabe and N. Kobayashi, Proceedings of 8th Internatinal Symposium on Superconductivity, (1995) to be published.
18) M. Tinkham, *Introduction to Superconductivity*, (McGraw-Hill, New York,1975)
19) H. Kitano, T. Shibauchi, K. Uchinokura, A. Maeda, H. Asaoka and H. Takei, Phys. Rev. B**51**, (1995) 1401.
20) Y. Iye, A. Fukushima and T. Tamegai, Physica C**185**, (1991) 297.
21) N. Kobayashi, K. Hirano, Y. Minagawa, T. Sasaki, K. Watanabe, S. Awaji, H. Asaoka and H. Takei, Physica C**235-240**, (1994) 2785